

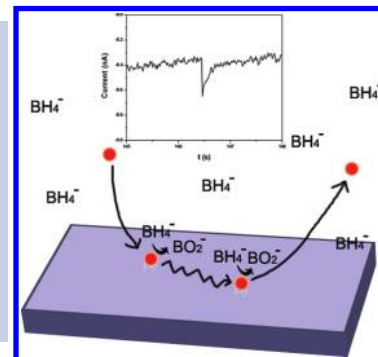
Observation of Discrete Au Nanoparticle Collisions by Electrocatalytic Amplification Using Pt Ultramicroelectrode Surface Modification

Hongjun Zhou, Fu-Ren F. Fan, and Allen J. Bard*

Center for Electrochemistry, Center for Nano and Molecular Science and Technology, Department of Chemistry and Biochemistry, University of Texas at Austin, 1 University Station A5300, Austin, Texas 78712-0165

ABSTRACT After growing a thin layer of oxide (PtO_x) by anodization of a Pt electrode, it changed from catalytically active for electrochemical NaBH_4 oxidation into an inactive electrode. When held at a potential where the oxide film was maintained, collisions of individual 14 nm diameter Au nanoparticles (NPs) that catalyzed NaBH_4 oxidation were successfully observed as discrete current pulses (spikes or blips) for each NP interaction with the modified Pt electrode via amplification from NaBH_4 oxidation. The current response is affected by NP concentration and the applied potential.

SECTION Nanoparticles and Nanostructures



Previous reports from this laboratory described a scheme to observe the currents caused by collisions of individual NPs at an electrode by electrocatalytic amplification.^{1–3} The protocol mainly involves three components, (1) choice of an inner sphere heterogeneous electron-transfer reaction,⁴ whose reaction kinetics strongly depend on the electrode material (e.g., proton reduction or hydrazine oxidation), (2) a colloidal solution of a low concentration ($\sim\mu\text{M}$) of NPs that are electrocatalytic for this inner sphere reaction, (3) an inert conductive ultramicroelectrode (UME), which, at the applied potential, shows essentially no electrocatalytic effect for this reaction.

The selection of electrode material is critical in observing NP collisions. To obtain a negligible current from the electrode at the applied potential, its electrocatalysis for the chosen reaction should be small; typically C or Au electrodes have been used. The detecting electrode must be an UME (radius $\approx\text{nm}$ to μm) to minimize collisions of more than one NP at a time and to obtain a good signal/noise ratio since the current that results from the collision of a single NP is very small. The NP must be a good electrocatalyst for the reaction, and Pt NPs have usually been used. Moreover, as we have found previously,^{1,2} the NP must be in contact with the electrode surface so that the residence times of NPs at the electrode surface are sufficiently long to allow the current from a single NP collision to be detected. Indeed in the previous studies, the particles stuck to the electrode; therefore, each showed a characteristic current step and an overall staircase response.

As shown in Scheme 1, we changed an active Pt electrode into one with an inactive surface by simply growing a thin layer of oxide via anodization. The oxide layer inhibited the inner sphere reaction on the Pt surface but still allowed electron tunneling, for example, to a NP from the solution, to take place.⁵ NaBH_4 was used as a heterogeneous inner

sphere reductant. Borohydride oxidation ($E^0 = -1.24$ vs NHE), as many other multielectron-transfer reactions,⁶ depends strongly on the electrode material.^{7–11} To suppress the hydrolysis of NaBH_4 , 10 mM NaBH_4 was dissolved in 0.1 M NaOH .¹² As shown in Figure 1a, the oxidation of NaBH_4 starts at negative potentials at both Au and Pt UMEs. The oxidation at the Pt UME occurs more easily (i.e., shows a negative shift in the onset potential by about 0.3 V) compared to the Au UME (region I). However, injecting Pt NPs and recording the current at a Au UME, following previous studies on hydrazine oxidation, only resulted in steady current increases with no distinguishable current steps from single NP collisions (Figure S1, Supporting Information). This inability to observe individual NP collisions has also been seen previously with other electrocatalytic systems (e.g., with Pt NPs stabilized with polyvinylpyrrolidone (PVP) on a Au electrode for hydrazine oxidation).

However, when the potential was scanned to more positive values, the current due to NaBH_4 oxidation at both Au and Pt UMEs decreased and dropped to near zero at potentials > 0.5 V (vs Ag/AgCl). This is caused by the gradual formation of adsorbed oxygen or oxide films on the metal electrodes. Oxidized Pt and Au are not electrocatalytic toward NaBH_4 oxidation, as with many other reactions that occur at the metal surface, for example, hydrogen oxidation. When the potential is scanned back in the negative direction, the oxidation current at a Au UME increases, starting at ~ 0.2 V (vs Ag/AgCl), but the oxidation current at a Pt UME remains near zero until ~ -0.25 V (vs Ag/AgCl) (region II in Figure 1a) because Au

Received Date: July 15, 2010

Accepted Date: August 24, 2010

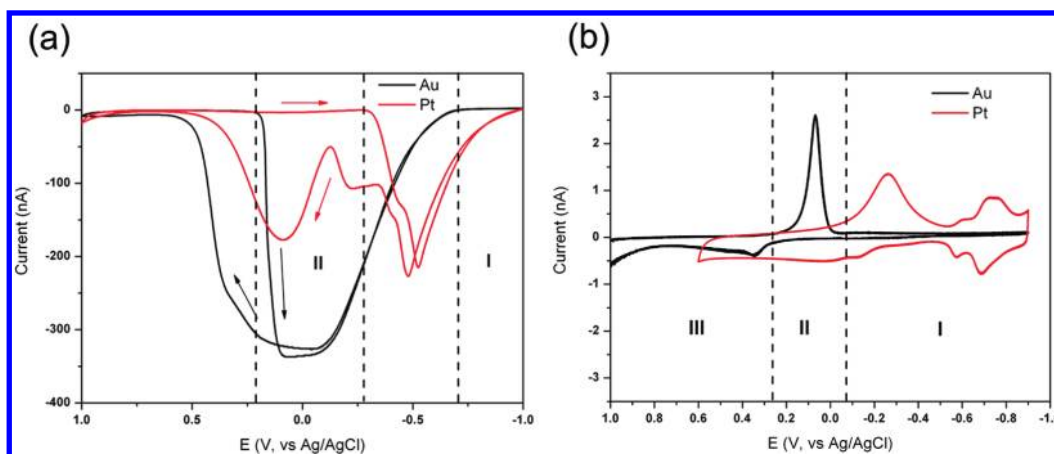
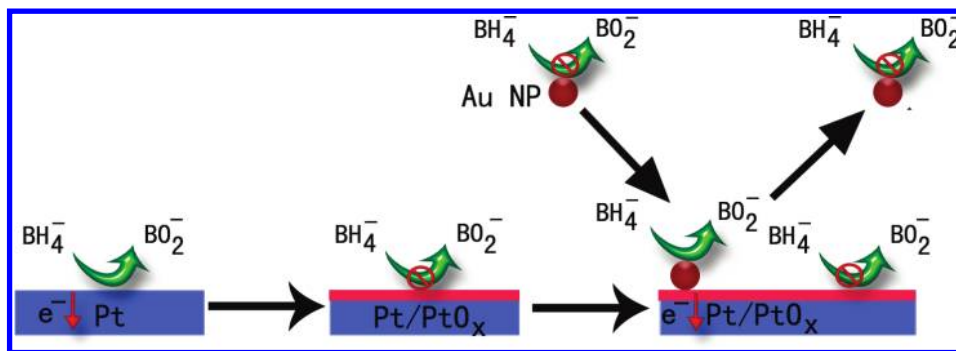


Figure 1. (a) Cyclic voltammograms of Au and Pt UMEs in a 10 mM NaBH₄, 0.1 M NaOH solution. (b) Cyclic voltammograms of Au and Pt UMEs in a 0.1 M NaOH solution. (Diameter of both UMEs, 10 μm; sweep rate, 100 mV/s.)

Scheme 1. Schematic of a Single Au NP Collision Event on a PtO_x-Covered Pt UME



oxide is easier to reduce than Pt oxide (Figure 1b). Thus, in region II, Au metal and Pt oxide are the stable forms. In this potential window, we could observe collisions of single Au NPs on an oxidized Pt UME.

We applied two rapid sequential potential steps to grow a Pt oxide layer (first step) and then observe collisions (second step). These two steps must be applied with no programmed delay between them, or else, the Pt oxide will be reduced by the NaBH₄ at the open circuit (i.e., the steady-state open circuit potential (OCP) of the Pt UME is always ~ -1 V in NaBH₄ solution). By contrast, in the absence of NaBH₄ in the 0.1 M NaOH solution, the OCP shifts positively depending on the thickness of the oxide layer (e.g., from -0.90 to 0.65 V after oxidation at 0.9 V for 10 s) and remains as a stable layer, for example, at 0 V, until electrochemically or chemically reduced.

Details of the experiments are given in the Supporting Information. Briefly, a Pt UME was first oxidized at 0.9 V (vs Ag/AgCl) for 10 s and then held at 0 V (vs Ag/AgCl) immediately followed by injection of the Au NPs, synthesized by the citrate reduction method.¹³ The presence of excess citrate in the solution does not introduce any new electrochemical peaks, as shown in Figure S2, Supporting Information, even at higher citrate concentrations. The average particle diameter was $\sim 14 \pm 0.5$ nm. TEM images and UV-vis spectra of these Au NPs are shown in Supporting Information Figure S3. The

number of Au atoms, n , in a NP ($\sim 84\,700$) was roughly calculated by the mass ratio of a NP and an atom, as shown in the equation below.

$$n = \pi \rho d^3 N_A / 6M \quad (1)$$

where ρ is the density of gold, d is the diameter of the Au NP, N_A is the Avogadro constant, and M is the atomic weight of Au. The Au NP stock solution contained about 4.7 μM particles. At the start of the measurement, an amount of Au NP stock solution that would produce a concentration of ~ 5 – 40 pM was injected into the solution. The solution was then stirred by bubbling Ar gas for 5–10 s to disperse the NPs. The current–time (i – t) response was recorded after lifting the Ar gas tube out of the solution.

Figure 2 shows a typical i – t curve (after 10 s) on a pre-oxidized (first 10 s) Pt UME before and after injection of the citrate-reduced Au NP solution. After oxidation at 0.9 V, the thin oxide layer on Pt blocked most of the active sites for NaBH₄ oxidation, resulting in a small background current (Supporting Information Figure S4). The surface oxidation state was estimated by calculating the ratio of the reduction charge of PtO_x (Q_O) and the hydrogen adsorption charge (Q_H) in a 0.1 M NaOH solution (Supporting Information Figure S5). After oxidation at 0.9 V for 10 s, the Q_O/Q_H was ~ 3.3 . The ratio of Q_O/Q_H increased at more positive potentials but remained

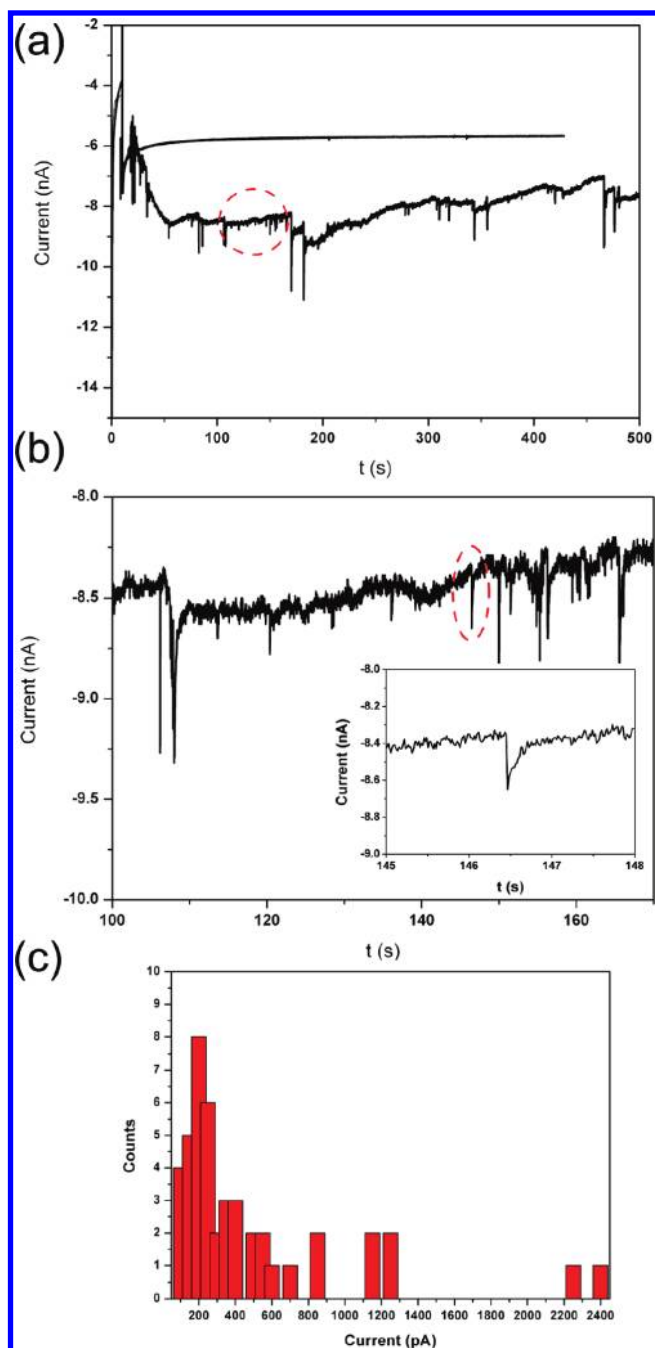


Figure 2. (a) The *i-t* curve without (upper curve) and with (bottom curve) injected Au NPs at the preoxidized Pt UME. UME diameter, 10 μm ; NP concentration, 24 μM ; potential, 0 V. (b) Zoom-in of the marked region in panel (a). The inset is a single-collision peak. (c) Statistical distribution of amplitudes of current peaks.

constant when the electrode was at open circuit in the absence of NaBH_4 . The ratio decreased very slowly when the electrode was held at 0 V after oxidation at 0.9 V, indicating that the PtO_x layer produced was stable in the NaBH_4 solution at 0 V (note that 0 V is still positive of the reduction peak of PtO_x in Figure 1b).

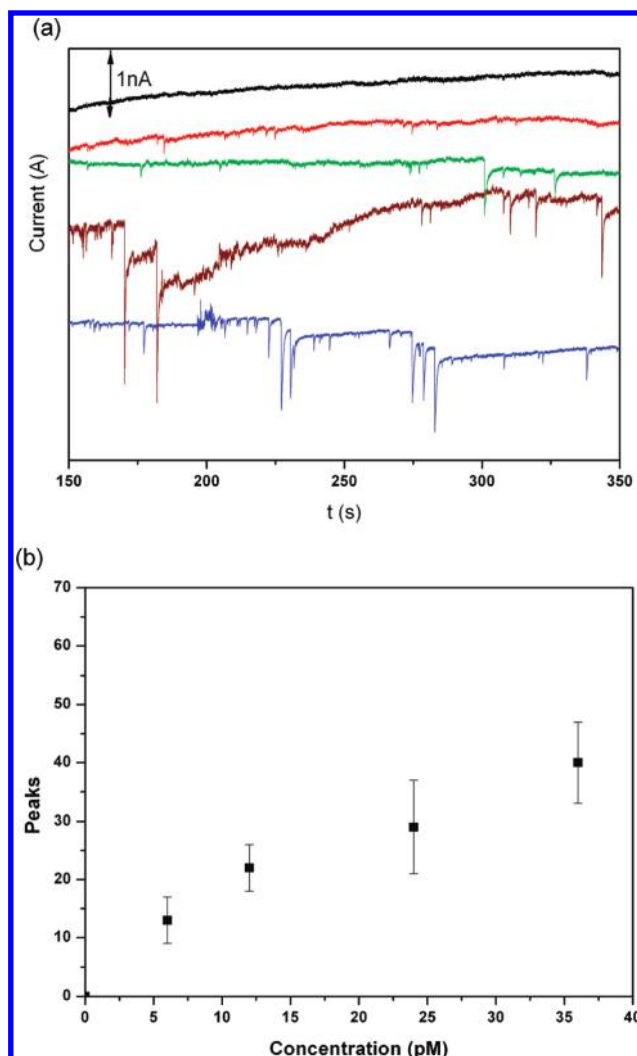


Figure 3. (a) The *i-t* curves recorded on a preoxidized Pt UME (10 μm) at 0 V in the presence of different concentrations of Au NPs, from top to bottom, 0, 6, 12, 24, and 36 μM . (b) Peaks counted in the time interval of 200 s at different concentrations; electrolyte, 10 mM; NaBH_4 , 0.1 M NaOH.

Once Au NPs contacted the Pt/ PtO_x electrode, the oxidation of NaBH_4 could occur on active sites of the Au NPs via electrons transferred by tunneling through this thin oxide film, providing the needed electrocatalytic amplification. Note that the Au NPs must be in contact with the electrode long enough so that the current observed is distinguishable from the background. However, the transient lasted only about 1 s, and the current then returned essentially to the background level (Figure 2). The individual current–time profile was affected by particle size, the particle residence time, and the nature of the interaction between the particle and the electrode surface. If NPs stuck to the electrode surface after collision, a steady-state current would be achieved for each NP, and the oxidation current would increase in a staircase response, as observed previously on Pt NP collisions.^{1,2} Here, the current profiles were more peak-like rather than steps, indicating the NPs leave or are deactivated after collisions.

Depending on the residence times of Au NPs on the electrode, a different amount of charge would be transferred; this determines the amplitudes of the peaks shown in Figure 2. Most of the peaks were in the range of 100–400 pA, which are smaller than the estimated steady-state diffusion-controlled current for a 14 nm Au NP to oxidize 10 mM NaBH₄, ~1 nA.² Several larger peaks >1 nA were seen, but these are probably collisions of aggregates of NPs. The charge transferred in a typical collision is around 4×10^{-11} C for a current peak of 300 pA, as shown in Figure 2b. This amount of charge is much higher than that to oxidize the whole Au NP (around $1.4\text{--}4 \times 10^{-14}$ C, assuming $n = 1\text{--}3$ per Au atom) or simply to charge the particle (about 1×10^{-16} C assuming a capacitance of $20 \mu\text{F}/\text{cm}^2$ and potential step of 1 V). Thus, these peaks originate from catalyzed NaBH₄ oxidation rather than the Au NP itself, which would not be distinguishable from the background.

To support the claim that these peaks are associated with collisions of Au NPs on the Pt/PtO_x UME, additional experiments were carried out. (1) The concentration of Au NPs in the solution was varied, and the frequency of the collision was found to be essentially proportional to the particle concentration (Figure 3); the frequency is roughly $0.01 \text{ s}^{-1} \text{ pM}^{-1}$. (2) After the UME was oxidized at 0.9 V, 50 pM Pt NPs (NaBH₄ reduced, citrate stabilized)¹⁴ were first injected, followed by injection of 20 pM Au NPs. No peaks appeared before injection of Au NPs (Supporting Information Figure S6). (3) The bias potential of a Au UME was varied from 0 to 0.6 V. As shown in Supporting Information Figure S7, the oxidation current strongly depended on the potential, which determines the extent of oxidation of the Au surface. At potentials > 0.4 V, the surface of Au was oxidized and lost electrocatalytic activity for borohydride oxidation. The oxidation currents dropped to almost 0. The collision peaks observed at different potentials agree well with this finding (Supporting Information Figure S8). With increasing potential, the peak heights decreased, and above 0.4 V, very few or no peaks were found.

In conclusion, collisions of single Au NPs on a modified electrode have been demonstrated. This approach combines the advantage of using Pt UMEs and Au NPs (probably the most studied metal NP). This greatly facilitates further investigations of the effects of particle size, shape, and stabilizing agent on the collision behavior. Moreover, Au NPs are of interest as labels because of their biocompatibility, tunable optical properties, and good control of size and shape.^{15,16} Preliminary experiments have been carried out using this strategy with other electrodes. For example, a thin film of Ni deposited on a Pt UME forms an oxide film and blocks NaBH₄ oxidation in 0.1 M NaOH but allows collisions of Pt NPs at 0 V (without previous oxidation) to be observed. Other strategies for surface and NP modification and alternative electrocatalytic reactions are currently under investigation.

SUPPORTING INFORMATION AVAILABLE Additional experimental data including a TEM image and UV–vis spectrum of Au NPs, as well as additional electrochemical and collision experiments. This material is available free of charge via the Internet at <http://pubs.acs.org>.

AUTHOR INFORMATION

Corresponding Author:

*To whom correspondence should be addressed. E-mail: ajbard@mail.utexas.edu. Tel: 512 471 3761. Fax: 512 471 0088.

ACKNOWLEDGMENT This work was supported by the National Science Foundation (CHE-0808927) and the Robert A. Welch Foundation (F-0021).

REFERENCES

- (1) Xiao, X.; Bard, A. J. Observing Single Nanoparticle Collisions at an Ultramicroelectrode by Electrocatalytic Amplification. *J. Am. Chem. Soc.* **2007**, *129*, 9610–9612.
- (2) Xiao, X.; Fan, F.-R. F.; Zhou, J.; Bard, A. J. Current Transients in Single Nanoparticle Collision Events. *J. Am. Chem. Soc.* **2008**, *130*, 16669–16677.
- (3) Xiao, X.; Pan, S.; Jang, J. S.; Fan, F.-R. F.; Bard, A. J. Single Nanoparticle Electrocatalysis: Effect of Monolayers on Particle and Electrode on Electron Transfer. *J. Phys. Chem. C* **2009**, *113*, 14978–14982.
- (4) Bard, A. J.; Faulkner, L. R. *Electrochemical Methods, Fundamentals and Applications*, 2nd ed.; John Wiley & Sons: New York, 2001.
- (5) Conway, B. E.; Tremiliosi-Filho, G.; Jerkiewicz, G. Independence of Formation and Reduction of Monolayer Surface Oxide on Pt from Presence of Thicker Phase-Oxide Layers. *J. Electroanal. Chem.* **1991**, *297*, 435–443.
- (6) Bard, A. J. Inner-Sphere Heterogeneous Electrode Reactions. Electrocatalysis and Photocatalysis: The Challenge. *J. Am. Chem. Soc.* **2010**, *132*, 7559–7567.
- (7) Mirkin, M. V.; Bard, A. J. Voltammetric Method for the Determination of Borohydride Concentration in Alkaline Aqueous Solutions. *Anal. Chem.* **1991**, *63*, 532–533.
- (8) Celikkan, H.; Sahin, M.; Aksu, M. L.; Veziroglu, T. N. The Investigation of the Electrooxidation of Sodium Borohydride on Various Metal Electrodes in Aqueous Basic Solutions. *Int. J. Hydrogen Energy* **2007**, *32*, 588–593.
- (9) Concha, B. M.; Chatenet, M. Direct Oxidation of Sodium Borohydride on Pt, Ag and Alloyed Pt–Ag Electrodes in Basic Media. Part I: Bulk Electrodes. *Electrochim. Acta* **2009**, *54*, 6119–6129.
- (10) Santos, D. M. F.; Sequeira, C. A. C. Chronopotentiometric Investigation of Borohydride Oxidation at a Gold Electrode. *J. Electrochem. Soc.* **2010**, *157*, F16–F21.
- (11) Liu, B. H.; Li, Z. P.; Suda, S. Anodic Oxidation of Alkali Borohydrides Catalyzed by Nickel. *J. Electrochem. Soc.* **2003**, *150*, A398–A402.
- (12) Liu, B. H.; Yang, J. Q.; Li, Z. P. Concentration Ratio of [OH⁻]/[BH₄⁻]: A Controlling Factor for the Fuel Efficiency of Borohydride Electro-oxidation. *Int. J. Hydrogen Energy* **2009**, *34*, 9436–9443.
- (13) Qian, L.; Gao, Q.; Song, Y.; Li, Z.; Yang, X. Layer-by-layer Assembled Multilayer Films of Redox Polymers for Electrocatalytic Oxidation of Ascorbic Acid. *Sens. Actuators, B* **2005**, *107*, 303–310.
- (14) Yang, J.; Lee, J. Y.; Too, H. P. Size Effect in Thiol and Amine Binding to Small Pt Nanoparticles. *Anal. Chim. Acta* **2006**, *571*, 206–210.
- (15) Nam, J.-M.; Thaxton, C. S.; Mirkin, C. A. Nanoparticle-Based Bio-Bar Codes for the Ultrasensitive Detection of Proteins. *Science* **2003**, *301*, 1884–1886.
- (16) Jain, P. K.; El-Sayed, I. H.; El-Sayed, M. A. Au Nanoparticles Target Cancer. *Nano Today* **2007**, *2*, 18–29.